# Application Research of an Array Distributed IMU Optimization Processing Method in Personal Positioning in Large Span Blind Environment

**HENGZHI LIU[1,2,3], QING LI[1,2,3], CHAO LI[3,4], AND HUI ZHAO[3,4]**

[1]School of Automation, Beijing Information Science and Technology University, Beijing 100192, China
[2]Institute of Intelligent Control, Beijing Information Science and Technology University, Beijing 100192, China
[3]Beijing Key Laboratory of High Dynamic Navigation Technology, Beijing Information Science and Technology University, Beijing 100192, China
[4]School of Automation, Beijing Institute of Technology, Beijing 100084, China

Corresponding author: Hengzhi Liu (liuhengzhi0279@gmail.com)

**ABSTRACT** Aiming at the long-term cumulative error inherent in pedestrian indoor inertial positioning filed, that error is mainly due to the low signal-to-noise ratio of the sensor output signal quality, the temperature drift of the gyro and the accuracy of error estimation. This paper proposes a new optimization method for array distributed MEMS-IMU: this method performs filtering and noise reduction optimization processing on inertial sensor data; The effect of temperature on the gyroscope is reduced by matrix-optimized layout, and distributed temperature compensation is performed for eight IMUs. We used MEMS-IMU worn on the foot finishing the data acquisition. Then improved a novel Pearson coefficient particle filtering method to finally complete the information fusion and positioning process in a blind environment (no beacon auxiliary information) high-precision personal large span (long time span, large distance span). The indoor positioning test results in the No. 6 Office Building of National Defense Science and Technology Park in Beijing Institute of Technology verify that the method has a horizontal error of only 6.23m (TTD ≈ 0.52%) during the horizontal span positioning which the total distance is about 1200m; In terms of vertical large-span positioning accuracy: the height error is only 4.56m (TTD ≈ 7.6%) during the positioning process of 68 minutes and 35 seconds (including intermediate stop). Compared with other multi-IMU personal positioning optimization methods, it has the advantages of high sensor data quality, small gyro temperature influence, good system error estimation accuracy and long-term long-distance positioning results. It provides a good and reliable theoretical reference for this field or extension applications.

**INDEX TERMS** Array distribution, MEMS-IMU, filtering noise reduction, optimized layout, multi-channel temperature compensation, improved Pearson coefficient particle filter, large span blind environment.

## I. INTRODUCTION

With the increasing autonomy of inertial components, personal positioning based on inertial components is a hot topic for extensive research. Currently, inertial measurement units are typically integrated into micro-electromechanical systems (MEMS) to provide a hardware foundation for wearable personal positioning terminals [1], [2]. In the indoors where the GPS signal is blocked, the personal positioning of the non-beacon pure inertial navigation has become the main technical means. The Draper laboratory in the United States first proposed to fix the MEMS-IMU on the foot at the end of

The associate editor coordinating the review of this manuscript and approving it for publication was Yue Zhang[ID].

the 20th century. Because the positioning unit is a single IMU module. Therefore, the data solution and positioning effect is not good. In order to improve the positioning effect, multi-channel IMU data fusion is now used to improve the accuracy [3], [4]. However, in the face of inertia components, there is an inevitable long-time drift cumulative error problem. And the positioning accuracy is limited in a large span blind environment. Therefore, the study of personal positioning in this environment has very important theoretical and engineering significance.

In terms of sensor data, it usually contains noise signals, which is unavoidable due to the hardware circuit and the sensor itself. The sensors' signal with noise will seriously affect data resolution accuracy and personal positioning

**IEEE** Access

H. Liu *et al.*: Application Research of an Array Distributed IMU Optimization Processing Method in Personal Positioning

result. So how to improve the data quality and effectively filter the noise is the first big problem to ensure the personal positioning effect in a large span blind environment [5]–[10]. Then the gyro sensor in MEMS-IMU has the characteristics of self-diffusion and random drift. At the same time, the external factors affecting the gyro sensor mainly come from the temperature [11]–[16]. While the main control arm chip on the circuit board of the positioning module is the main heat source for a long time working. So how to properly arrange the heating arm chip and IMU to form a good heat dissipation space, improve the overall reliability and stability of the system is the second major problem that needs to be solved [17]–[25]. The existing pedestrian navigation filter mainly uses Kalman filter. It solves the linear problem with good effect and can accurately estimate the systematic error [26], [27]. But the pedestrian navigation data is purely nonlinear. The extended Kalman filter (EKF) is applied to calculate it. It can only solve the non-linear systems with the linear characteristics. So how to solve the navigation data error estimation of purely nonlinear systems is the third problem [28]–[30]. The existence of the above three major problems are mainly due to the influence that positioning with long-time and long-distance, and the performance declines in such environment significantly. Therefore, the above problems have become a technical bottleneck and a research hotspot by experts and scholars in this field.

In order to suppress the drift error of the MEMS gyro, we usually adopt the method of filtering after modeling. And the compensation effect depends on the accuracy of the modeling and the effect of filtering. An adaptive method that weighs the range, the sampling frequency, and the output frequency is proposed and achieved good results to make full use of the sensor and to improve the output efficiency. Differential average median filtering method also achieved good results in sensor use and signal processing [9], [10]. The random drift of MEMS gyroscopes has non-stationary and nonlinear problems. Wavelet theory has been widely studied for the processing of non-stationary signals. Many scholars have made a lot of explorations on wavelet thresholds and achieved a lot of results [24], [25]. At the same time, the classic FIR and IIR filters are also applied in engineering to improve the gyro data quality. The research on the layout of printed circuit board components mainly focuses on optimizing the thermal conductive material and the average material parameters to improve the thermal conductivity and reduce the heating temperature. In the thermal resistance analysis of printed circuit boards, the fixed resistance is usually used for analysis. Different resistance values are used to select the placement position of the components [9]–[12]. Particle filtering has been widely used in solving nonlinear non-Gaussian models. It is usually used to eliminate particles with small weights and replicate weights to eliminate particle degradation. The research direction of particle filtering focuses on re-sampling. At present, the main methods are Polynomial sampling, system re-sampling, residual re-sampling, layered re-sampling, etc. [29], [30].

On the basis of some achievements in the above research, there are still some problems to be solved: the FIR filter has good stability and linear phase characteristics. But due to its high order, there is a problem of large delay; One disadvantage of the IIR filter in designing is that the phase characteristics of the filter cannot be controlled, which will make the filter unstable; the wavelet threshold filter has good stability and real-time. But there are always local oscillations and certain deviation from the actual signal due to the threshold itself; some researchers optimize the thermal conductivity of the printed circuit board material and raise the heat dissipation level, which leads to the lapse of the component's basic performance. The method of fixing the thermal resistance does not truly reflect the heat release distribution of the printed circuit. The layout based on that does not optimize the heat dissipation effect; the commonly used method in particle filtering leads to the lack of particle diversity after resampling, which also brings about the problem of particle depletion.

In this paper, an optimized processing method for array distributed IMU in personal positioning is proposed. The filtering and noise reduction method based on adaptive threshold sequence of genetic algorithm can effectively extract and eliminate noise signals, which solves the delay, instability and fixedness error of the general method. Then it improves the sensor data quality; the Fourier series is introduced to analyze the thermal resistance distribution of the printed circuit board. And the eight IMUs are rationally laid out on the board of ensuring the working performance of the components. Then reasonable temperature compensation for each IMU has improved the navigation data quality. On the basis of the common particle filtering method, we proposed the particle filter algorithm of Pearson coefficient. The particle selection uses the Pearson coefficient function to obtain the surrounding particles and channels with larger weight values for being closer to the real system. It can effectively solve the problems of particle degradation and particle depletion.

The specific technical flow chart is shown in the following figure:

## II. PRE-PROCESSING AND OPTIMIZATION OF LAYOUT
### A. FILTERING NOISE REDUCTION PREPROCESSING
There is a large random error in the initial data of the inertial device. Through preprocessing, the quality of the inertial navigation data can be obtained, which provides a good data foundation for the navigation result output. In this paper, an Genetic Adaptive threshold sequence Filtering Noise-reduction (GAFN) algorithm is proposed. Based on the traditional genetic algorithm, the optimized binary multiplication sequence is added. Through the time-frequency conversion and the similarity comparison, the optimal time-domain inertial data after filtering noise-reduction is obtained. This method is not currently applied in the field of inertial navigation, and it can simultaneously handle the multi-dimensional inertial data solution (x, y, z-axis) to improve efficiency and effect.

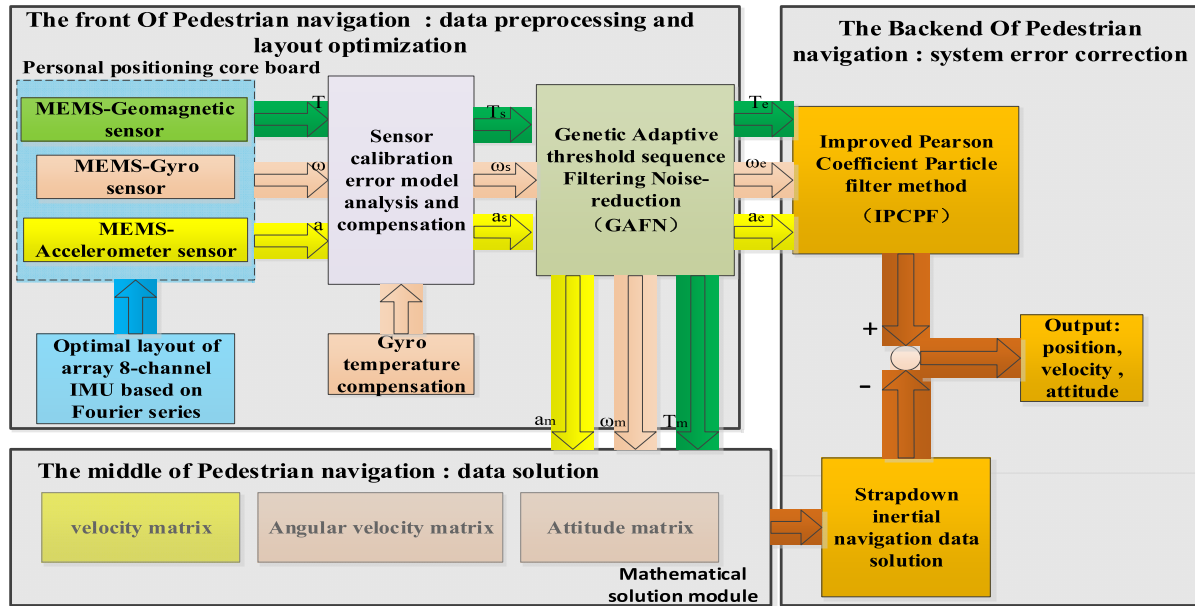H. Liu *et al.*: Application Research of an Array Distributed IMU Optimization Processing Method in Personal Positioning

IEEE*Access*



**FIGURE 1.** Technical schematic.

### 1) TRADITIONAL GENETIC ALGORITHM PRINCIPLE

The principle of genetic algorithm is to simulate Darwin's genetic selection and the computational model of the biological evolution process of natural elimination. It is a method to search for the optimal solution by simulating the natural evolution process. The genetic algorithm starts from the potential solution set that solves the problem. Each solution set is composed of multiple individuals encoded by the gene sequence, and each individual's chromosome is an entity with model features. As the main carrier of genetic characteristics, chromosomes can be composed of multiple genes. The internal representation is a combination of gene codes, and the external representation is the trait of the output. Due to the complexity of human genes, there is no way to reproduce through code. In order to simplify the operation of gene coding, the binary code is used to simulate the gene sequence coding. After the initial generation solution is generated, it follows the principle of survival of the fittest evolves from generation to generation and continues to inherit the superior characteristics of the father for the final required output result (the optimal solution set). In each generation, we select individuals according to the degree of fitness of the individual in the problem domain. Then we combine them with the genetic operators of natural genetics to generate crossovers and variations for a solution set that is more in line with the needs. This process will lead to the fact that the epigenetic solution set like the natural evolution is more adaptive to the optimal result than the previous generation. And it will get the optimal solution set.

### 2) ADAPTIVE THRESHOLD SEQUENCE (ATS)

Chromosomes are important trait carriers in inheritance. They determine the direction in which humans or animals develop.

Similarly, adaptive threshold sequences (ATS) in adaptive filters are similar to chromosomes, and ATS are also a key part of filters. The ATS is mainly used to multiply the original noise signal. In order to extract the part that meets our requirements. Then we retain the features of the part in the sequence, and genetically improve the parts that do not meet the requirements. After multiple iterations, the optimal sequence is reached. Thereby output the desired signal.

Under different baud rates, the amount of signal data collected per unit time is different. Taking the baud rate of 921600 as an example: under one hour of experimental time, the amount of inertial output data is as high as 1.5 million data points. After the fast Fourier transform of the signal, the adaptive sequence cannot directly generate 1.5 million binary codes. Therefore, an extended binary adaptive sequence is used. Experiment with the same inertial navigation at the same time as the baud rate of 3600, we can get 5860 data points under that condition. In other words, the sequence is composed of 5860 binary codes firstly. And then each binary code as a module to be expanded 256 times. Each of the elements of the module contained the same value.

*Adaptive threshold strings*

$$= \begin{bmatrix} 0 & 1 & \dots & 1 & 1 \\ 0 & 0 & \dots & 0 & 1 \\ \dots & \dots & \dots & \dots & \dots \\ 1 & 1 & \dots & 0 & 0 \\ 0 & 1 & \dots & 0 & 1 \end{bmatrix} \quad \textit{extend to}$$

$$\times \begin{bmatrix} 00\dots00 & 00\dots00 & \dots & 11\dots11 & 00\dots00 \\ 11\dots11 & 00\dots00 & \dots & 00\dots00 & 11\dots11 \\ \dots & \dots & \dots & \dots & \dots \\ 11\dots11 & 11\dots11 & \dots & 00\dots00 & 00\dots00 \\ 00\dots00 & 11\dots11 & \dots & 00\dots00 & 11\dots11 \end{bmatrix}$$

We can see from the above formula: it can be consistent with the data length of the baud rate of 921600 after expansion. And it can simplify the calculation and improve the system efficiency in the subsequent sequence optimization process.

We discuss how the quantity composition of the ATS is formed. The basic principle of relying on genetic algorithms for how to take values in adaptive threshold sequences: the generation of the first sequence is random. And after a genetic operation, we acquire the excellent features of this generation and retain it. The evaluation of good features depends on the similarity of the signal with each genetic operation and static data noise. The dynamic threshold process of similarity improvement is the adaptive sequence optimization process.

### 3) PRINCIPLE OF GAFN ALGORITHM

The GAFN algorithm actually performs the process of genetic optimization and similarity comparison. Because the noise characteristics of the gyro sensor in the stationary state are obvious, the gyro noise signal in the static state is selected as the reference. In order to improve the gyro signal quality of pedestrian movements, the gyro noise in the motion state is the main processing object of the filtering noise-reduction algorithm. First, the fast Fourier transform is performed on the gyro data with noise in the motion state. The purpose is to convert the continuous data into point values for reducing the calculation amount of multiplication. Then, the first genetic operation is performed, and a binary sequence C is randomly generated. The binary sequence is mainly used for genetic operations, and the noise point value is extracted by multiplying the result of the fast Fourier transform. Then, the inverse fast Fourier transform is performed, and the extracted noise signal is transformed into a continuous signal representation and compared with the noise signal of gyro in the stationary state. If the similarity is not satisfied, the return genetic operation continues to optimize the binary sequence. If the similarity is satisfied, the optimized binary sequence is to be inverse. Finally, the inverse sequence is multiplied by the gyro noise after the fast Fourier transform of the motion state to complete the entire filtering noise-reduction process. The schematic is shown in Figure 2.

The measurement conditions for noise similarity are: (1) the phase similarity of the stationary state signal; (2) the amplitude similarity of the stationary state signal; (3) the reliability similarity of the stationary state signal (whether there is significant drift or divergence, etc.). The way to measure the reliability similarity is that the similarity of the probability and the frequency density distribution should be as high as possible.

The following is a mathematical model representation of the overall algorithm:

1) Static data noise: $x_s(t) = (x_s(t_1), x_s(t_2), \ldots, x_s(t_n))$
2) Dynamic data noise: $x_m(t) = (x_m(t_1), x_m(t_2), \ldots, x_m(t_n))$
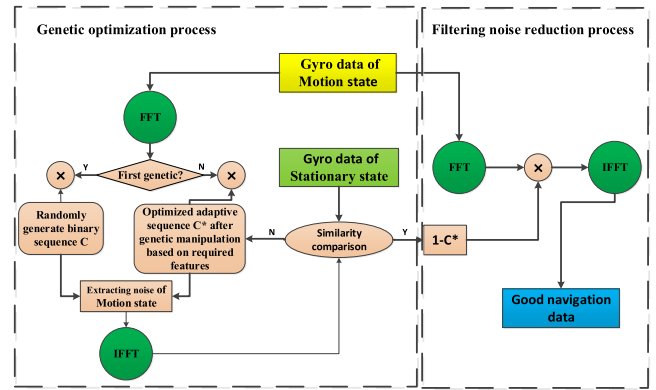3) Dynamic data noise after fast Fourier transform of dynamic data: $x_m(t) \xrightarrow{fft} x_m(f)$



**FIGURE 2.** The noise reduction of adaptive threshold sequence filtering based on genetic algorithm.

4) Randomly generate sequence C: $C = \{0, 0, \ldots, 0, 1, 0, \ldots, 0, 1, 0, \ldots, 0\}$
5) Random sequence C multiplied by $x_m(f)$ to get $x_m^*(f)$
6) Perform an inverse fast Fourier transform on the product result: $x_m^*(f) \xrightarrow{ifft} x_m^*(t)$
7) Perform similarity comparison on the results in (6). If the similarity does not meet the requirements, perform multiple genetic operations optimization on the random sequence C to generate an optimal sequence $C^*$. And use the product of $1 - C^*$ and the dynamic signal to select the true dynamic signal after noise-reduction.

The mathematical model for evaluating similarity is expressed as follows:
$a_j = \frac{1}{\pi}\sqrt{\int_0^\infty (2\pi t)^2 A_x(t)dt / \int_0^\infty A_x(t)dte^{-j^2/2\sigma_x^2}}$ represents the probability density distribution.

$$
\begin{aligned}
b_j &= \frac{1}{\pi}\sqrt{\int_0^\infty (2\pi t)^2 A_x(t)dt / \int_0^\infty A_x(t)dte^{-j^2/2\sigma_x^2}} \\
&\quad \times \sqrt{2\pi}/2 \int_0^\infty (2\pi t)^2 A_x(t)dt \\
&= a_j\sqrt{2\pi}/2 \int_0^\infty (2\pi t)^2 A_x(t)dt
\end{aligned}
$$

represents the frequency density distribution.

The similarity distribution can be obtained by combining the probability density and the frequency density distribution:

$$
\begin{aligned}
I_{ab} &= \sum_{j=1}^n \log\left\{(a_j^*/a_j) \times (b_j^*/b_j)\right\}/n \\
&= \sum_{j=1}^n \log\left\{(a_j^*/a_j)\right\}/n + \sum_{j=1}^n \log\left\{(b_j^*/b_j)\right\} \\
&= I_a + I_b
\end{aligned}
\tag{1}
$$

### B. ARRAY TYPE IMU OPTIMIZED LAYOUT

At present, the heat dissipation methods for PCB board mainly include thermal convection (small integrated circuit board is not commonly used) and natural convection (commonly used for small integrated circuit board). The chips and

H. Liu *et al.*: Application Research of an Array Distributed IMU Optimization Processing Method in Personal Positioning

IEEE *Access*

components of the pedestrian positioning terminal, we all use low-power devices. And the heat source of the pedestrian positioning terminal is mainly from the ARM chip STM401, so the reasonable thermal layout of the STM401 becomes the key to solving the thermal problem of the pedestrian positioning terminal. Placement of STM401 in the most reasonable place for natural convection can effectively dissipate heat, so that the entire terminal works at a reasonable working temperature. Thereby, it will improve the system accuracy, reduce the system errors and enhance the terminal's reliability.

### 1) LAYOUT MODEL DESCRIPTION

The real-time output of the thermal resistance is a transient value that cannot be directly analyzed. So the thermal model is analyzed by the average thermal resistance. Research on high-power and multi-chip module (MCM) has become a hot spot in the field of chip thermal analysis. But some research methods use fixed-value assumptions for thermal resistance when solving thermal analysis, which has caused certain errors and irrationalities in the thermal analysis model. The error is unreasonable. Therefore, this paper proposes a method of expanding the thermal resistance with Fourier series to ensure the true reliability of the thermal resistance analysis. For the model with a large amount of heat, only a few parameter conditions need to be considered due to the fast convergence of the thermal resistance expansion.

The steady state equation of the system can be expressed as

$$\nabla^2 T = \frac{\partial^2 T}{\partial x^2} + \frac{\partial^2 T}{\partial y^2} + \frac{\partial^2 T}{\partial z^2} \tag{2}$$

Only the heat dissipation caused by the heat convection is considered, so the boundary condition of the following equation can be expanded by the Fourier series.

$$\frac{\partial T}{\partial z}\bigg|_{z=t} = -\frac{h}{k}\left[T(x, y, t) - T_f\right] \tag{3}$$

Expanding the boundary condition with a Fourier series

$$\theta(x, y, z) \equiv T(x, y, z) - T_f$$
$$= A_0 + B_0 z + \sum_{m=1}^{\infty} \cos(\lambda_m x)\left[A_m \cosh(\lambda_m z)\right.$$
$$\left. + B_m \sinh(\lambda_m z)\right] + \sum_{i=1}^{\infty} \cos(\delta_n y)\left[A_m \cosh(\delta_n z)\right.$$
$$\left. + B_m \sinh(\delta_n z)\right] + \sum_{m=1}^{\infty}\sum_{n=1}^{\infty} \cos(\beta_{mn} z)\cos(\beta_{mn} z)$$
$$\times \left[A_{mn} \cosh(\beta_m z) + B_{mn} \sinh(\beta_m z)\right] \tag{4}$$

where $\lambda_m = m\pi/a$, $\delta_n = n\pi/b$, $\beta_{mn} = \sqrt{\lambda_m^2 + \delta_n^2}$.

The thermal layout optimization of the circuit board in the pedestrian positioning terminal is to find the variable that affects the temperature distribution. In other words, we will find the position of the heat-generating chip and the amount of the heat generation to minimize the value of the thermal resistance R.

The average temperature difference of a single STM32F401 can be expressed as

$$\bar{\theta} = \frac{1}{A}\iint_A \theta(x, y, 0)dA = RQ \tag{5}$$

Since the heating chip of the pedestrian navigation module has only one piece, the thermal resistance formula can be written as

$$R_S = \sum_m \frac{2}{\lambda_m \varphi(\lambda_m)} \cos^2(\lambda_m X_C) \sin^2 c(\lambda_m c/2) \tag{6}$$

The calculation of the optimal position of the pedestrian navigation heat source chip can be expressed as

$$F(\lambda_m) = \frac{2R_S}{\lambda_m \varphi\lambda_m} \tag{7}$$

Then we can get $R_S = \sum_m F^i(\lambda_m)$.

In order to minimize the thermal resistance value, it is necessary to minimize each item in the Fourier expansion formula of the thermal resistance value. Therefore, only taking the minimum value of the one that has the greatest influence in the expansion formula, that is the optimum minimum value of the thermal resistance.

According to the actual size of the existing personal positioning terminal: the length, width and height of the bottom plate are 0.03m, 0.018m and 0.0015m; and the length, width and height of the heat generating unit chip are 0.016m, 0.016m and 0.0001m. We performed simulation of the optimal position calculation. The simulation content mainly includes: the simulation of the Fourier series expansion formula of the thermal resistance; the influence of different parameters λ (first four items) on the thermal resistance system; the relationship between the chip size and the F value of the Fourier series; and the contour distribution of the Fourier series of chip positions under different parameters λ (first four items).

1) Simulation of Fourier series expansion formula of thermal resistance

As shown in Fig. 3, the F value rapidly decreases with the increase of m and approaches zero. It can be seen that when solving the thermal resistance of the positioning terminal, only the influence of the first few items needs to be considered.

2) Influence of different parameters (first four items) on thermal resistance system

It can be determined from Fig. 3 that the main factors affecting the thermal resistance are derived from the first few terms of the Fourier series expansion. So the selection of the optimal position should minimize the influence of the largest term. As can be seen from Fig. 4, Lamda1 has the greatest impact on the Fourier series F value. At X = 0.015m, it can be seen that lamda1 approaches 0, so the optimal position can be chosen to be 0.015m.

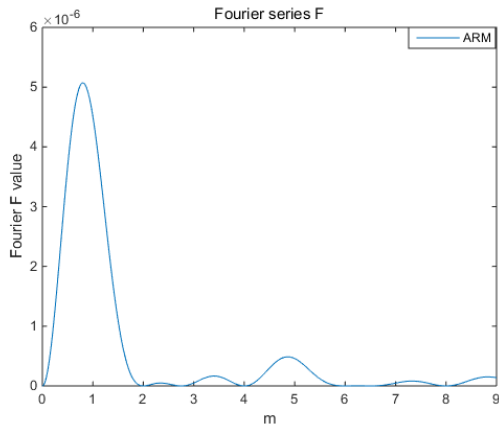3) Relationship between chip size and Fourier series F value

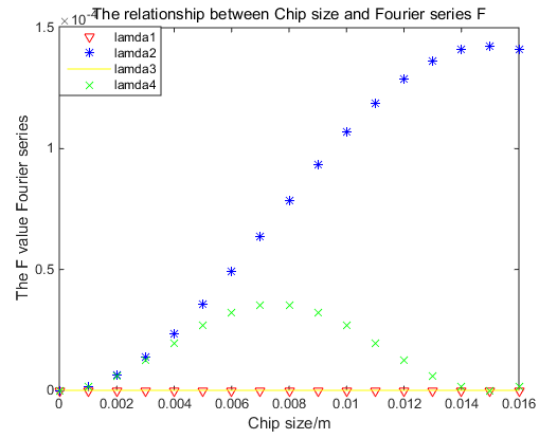**FIGURE 3.** The F map of thermal resistance Fourier series.



**FIGURE 4.** Under different positions: the influence of parameter on the thermal resistance Fourier series F.



**FIGURE 5.** Under different chip sizes: the influence of parameter lamada on the thermal resistance Fourier series F.
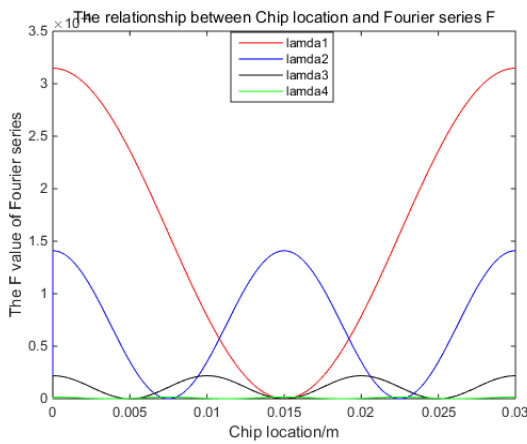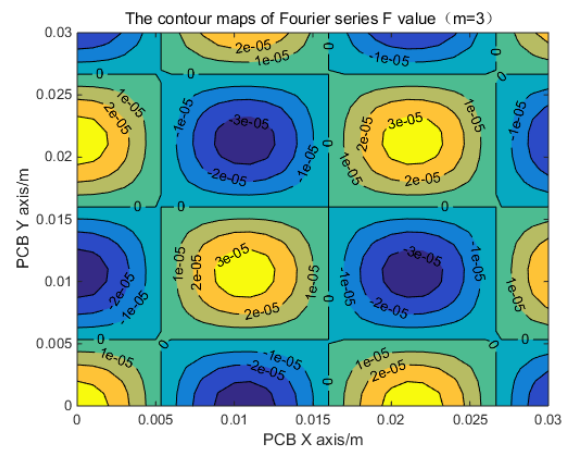


**FIGURE 6.** Thermal resistance distribution simulation contour map.

It can be seen from Fig. 4 that best position for thermal resistance selection is at X = 0.015m. After determining the optimal position, the optimal chip size is discussed. As can be seen from Fig. 5, when the chip is 0.016 m in length, the most influential lamda2 is close to the maximum value. That happens to be the size of the chip currently used. If you can choose the optimal size of the chip, of course, it will help to reduce the thermal resistance. But if you can't change it, choosing the optimal position is the most effective way to reduce the thermal resistance.

4) Fourier series contour distribution of chip position under different parameters lamda (first four terms)

Through the above analysis, a contour map of the chip position at different parameters lamda is established to determine the optimal positions of a single chip or a plurality of chips. Because the MPU9250 is a low-power sensor, it generates less heat for a long time. Considering its layout position, the 8 IMUs are arranged on the front and back of the circuit board, and the position which four thermal resistance contour lines are 0. STM32F401 is the main heating element, it is placed on the front center of the circuit board and the position with intersection of the zero thermal resistance contour lines.

By optimally selecting the reasonable position and size of the chip, the thermal resistance is reduced as much as possible. It can be seen from the above analysis and simulation that the optimal position has a cosine wave characteristic. Therefore, the wave node may be a suitable position. On the other hand, the optimal chip size has a basic sinusoidal characteristic of monotonic attenuation. The basic laws found in these simulations have greatly helped determine the minimum thermal resistance.

2) OPTIMIZATION RESULTS AND MULTI-CHANNEL TEMPERATURE COMPENSATION

On the basis of the above, the thermal stability analysis of the existing positioning terminal integrated circuit board through ANSYS. Because of the thermal steady state analysis, only the thermal conductive materials are divided into three categories in the simulation process: STM401 as the heat source of the circuit board; the plate body with thermal anisotropy; and other components that are not heat-generating. The material parameters are set as follows: the thermal conductivity of the integrated chip is uniformly 5 W/(m·°C); the thermal conductivity anisotropy of the printed board is 8.37, 8.37 and
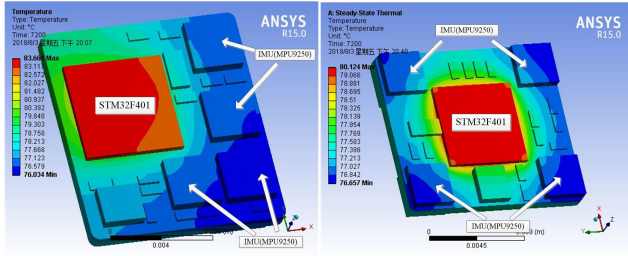
**FIGURE 7.** ANSYS thermodynamic layout simulation renderings.

0.32 W/(m·°C) respectively; and the device thermal conductivity is 1 W/(m·°C). The simulation time is set to 2 hours.

The initial finite element model of the electronic device uses free meshing. Each integrated chip transfers heat through conduction and obeys the Fourier heat transfer law. We take the ambient temperature at 30 °C, and consider the STM401 chip as a heat source. The formula for the heat generation rate q (W/m3 ) of the component is as follows:

$$q = \frac{P}{L \times W \times H} \quad (8)$$

where P is the component power consumption; L is the component length; W is the component width; and H is the component thickness.

It can be seen from Fig. 7 that the finite element thermodynamic analysis is performed according to the optimal position by changing the model parameters. After the optimal layout, the maximum temperature of the core plate is reduced by 3.537 °C, which is 4.23% lower than the before optimization's. And the average temperature is reduced by 2.83 °C. This shows that the optimized layout by Fourier series has a good cooling effect.

The zero drift of the gyro is mainly affected by various factors of the starting time and the temperature under the stable working state. So the gyro zero drift is compensated from these two directions.

The relationship between the resonant frequency of the gyro and temperature:

$$\omega_n(T) = \sqrt{K/m} = \sqrt{K_0(1 - k_{ET}(T - T_0)/m)} \quad (9)$$

In the small range around the temperature T0, the above equation can be approximated as:

$$\omega_n(T) = \omega_n(T_0)[1 - 1/2k_{ET}(T - T_0)] \quad (10)$$

Establish the gyro zero drift model, where $W_{ZO}$ is zero drift, $W_{S1}$ is the starting zero offset, and $W_{S2}$ is the stable zero offset:

$$W_{ZO} = W_{S1} + W_{S2} \quad (11)$$
$$W_{S1} = a_0 + a_1 t + a_2 t^2 \quad (12)$$
$$W_{S2} = a_0 + a_1 t + a_2 t^2 + a_3 T + a_4 T^2 + a_5 T^3 + a_6 T^4 + a_7 \Delta T \quad (13)$$

From the above, the zero offset compensation model of the MEMS gyro in the full temperature interval can be obtained

as follows:

$$W_{ZO} = \begin{cases} W_{S1} = a_0 + a_1 t + a_2 t^2, & t \le 600 \\ W_{S2} = a_0 + a_1 t + a_2 t^2 + a_3 T + a_4 T^2 + a_5 T^3 \\ \quad + a_6 T^4 + a_7 \Delta T, & t \ge 600s \end{cases} \quad (14)$$

By establishing the temperature compensation model of the MEMS gyro at the full temperature range, reasonable temperature compensation can be performed at the starting time and in the stable working period respectively, which can effectively ensure the measurement effect of the array type IMU gyro during those stages. After temperature compensation, it can be seen from Fig. 8 that between 40 °C and −20 °C, the gyro drift in the startup phase and the normal working phase is suppressed. It indicates that the compensation effect based on the above temperature compensation model is good. In a way, the problem that the gyro drift is large under long working hours is improved.
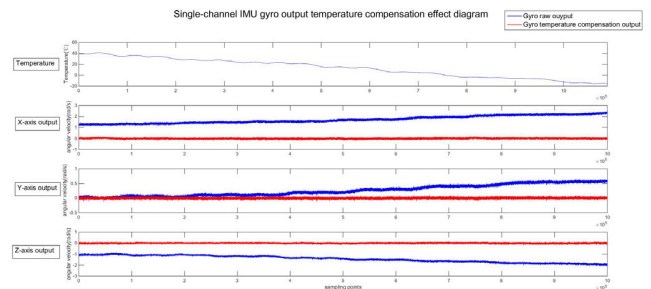


**FIGURE 8.** Single IMU temperature compensation effect diagram.

## III. IMPROVED PEARSON COEFFICIENT PARTICLE FILTER METHOD
### A. BRIEF DESCRIPTION OF THE CONCEPT
The traditional Kalman filter algorithm is mainly applied to linear systems. The extended Kalman filter applied to nonlinear systems also requires the system to be approximately linear. Therefore, it is necessary to use a filtering algorithm for pure nonlinear systems in pedestrian navigation field effectively solving that problem. We found that the particle filtering can solve this problem well. It is a special Bayesian filter based on Monte Carlo resampling method, which calculates the posterior probability density by randomly sampling the point value and the weight of the sample point. The particle filtering consists of three steps: (1) generating a new set of particles; (2) calculating the weight of the particles; (3) and the resampling process. The variance of the weight will increase as the number of iterations increases. That is, after multiple iterations, the weight of most particles will tend to zero. It is the so-called sample degradation in this research field. This problem will lead to multiple meaningless calculations in the subsequent iterative operation. And the obtained posterior probability density function will be distorted due to the decision of a small number of particles with the large weight. For this problem, the resampling process is usually

**IEEE** Access®

H. Liu *et al.*: Application Research of an Array Distributed IMU Optimization Processing Method in Personal Positioning

used. We eliminate particles with the small weights and copy particles with the larger weights to ensure the quality of the output.

### B. INNOVATION AND REALIZATION

#### 1) BUILDING THE BAYESIAN MATHEMATICAL MODEL SYSTEM MODEL

$$\begin{cases} x_k = f_k(x_{k-1}, v_{k-1}) \\ y_k = h_k(x_k, n_k) \end{cases} \quad (15)$$

Prediction process:

$p(x_k | y_{1:k-1})$ is obtained from the probability density $p(x_{k-1} | y_{1:k-1})$ at the previous moment. The meaning of this formula is: since there is measurement data from the previous 1 to k-1 moments, it is possible to predict the probability of the occurrence of the state $x(k)$.

Calculation derivation:

$$p(x_k | y_{1:k-1}) = \int p(x_k, x_{k-1} | y_{1:k-1}) dx_{k-1}$$

$$= \int p(x_k | x_{k-1}, y_{1:k-1}) p(x_{k-1} | y_{1:k-1}) dx_{k-1}$$

$$= \int p(x_k | x_{k-1}) p(x_{k-1} | y_{1:k-1}) dx_{k-1} \quad (16)$$

#### 2) BUILDING THE MONTE CARLO MATHEMATICAL MODEL UPDATE PROCESS

$$E(f(x)) = \int_a^b f(x) p(x) dx \quad (17)$$

$$Var(f(x)) = E(f(x) - E(f(x)))^2$$

$$= \int_a^b (f(x) - E(f(x)))^2 p(x) dx \quad (18)$$

Integral is used in the calculation of Bayesian posterior probability. In order to solve this difficult problem, Monte Carlo sampling can be used instead of calculating the posterior probability.

Use the mean value instead of the integral:

$$E(f(x)) \approx \frac{f(x_1) + \ldots + f(x_N)}{N} \quad (19)$$

The calculation of the posterior probability estimate can be expressed as:

$$\widehat{p}(x_n | y_{1:k}) = \frac{1}{N} \sum_{i=1}^N \delta(x_n - x_n^{(i)}) \approx p(x_n | y_{1:k}) \quad (20)$$

#### 3) CALCULATING THE PEARSON COEFFICIENT FUNCTION

The Pearson coefficient function calculates the values of $(x_k - \bar{x})$ and $(y_k - \bar{y})$ corresponding to $(x_k, y_k)$ in each sample. Where $\bar{x}$ and $\bar{y}$ represent the mean of $(x_k, y_k)$, respectively. The Pearson coefficient function can be expressed as follows:

$$S_{xy} = \frac{\sum (x_k - \bar{x}) \sum (y_k - \bar{y})}{\sqrt{\sum (x_k - \bar{x})^2 \sum (y_k - \bar{y})^2}} \quad (21)$$

When judging the change trend of the state variables and the observation variables, the value of $(x_k - \bar{x})(y_k - \bar{y})$ is

used as a reference. If the product is positive, it means that the state variables is consistent with the change trend of the observation variables; if the product is negative, it means that the state variables is opposite to the change trend of the observation variables. The product of each time point in the sample reflects the change trend correlation of the sample population. The value of the Pearson coefficient function $(S_{xy} \in [-1, 1])$ reflects the strength of the correlation of the sample change trend. When it is greater than 0, it indicates that the observation variables is positively correlated with the state variables; when it is less than 0, it indicates that the observation variables is negatively correlated with the state variables; when the absolute value of $S_{xy}$ is close to 1, it indicates that the observation variables has a strong correlation with the state variables.

The Pearson coefficient function can be used to understand the change trend of observations and states. If the observed path of the particle is close to the observed path of the true state in the system (the observed noise is small), the particle can be considered close and can track the true state of the system well. Calculate the degree of similarity between the two observation paths to determine whether the particles are close to the true state of the system. When the similarity coefficient is close to 1, it indicates that the particle is close to the real state of the system; otherwise, it indicates that the particle is far from the true state of the system. Therefore, particles can be selected by the Pearson coefficient function in order to obtain higher estimation accuracy.

#### 4) RE-SAMPLING PROCESS

In the re-sampling process, the transfer function in traditional particle filter is still used as the importance density function, as shown below.

$$x_k^i \sim P(x_k | x_k^i), \quad i = 1, \ldots, N \quad (22)$$

Re-randomly picking several new particles around each highly correlated particle:

$$x_k^i \xrightarrow{choose} x_k^{i,m}$$

where $x_k^i$ represents a highly correlated particle; and $x_k^{i,m}$ represents the newly selected particle around $x_k^i$.

Then calculate the Pearson coefficient values of these particles to select the particle path closest to the real state.

$$S_k^{i,m} = \frac{\sum_{k=1}^n (y_k^{i,m} - \overline{y^{i,m}})(y_k - \bar{y})}{\sqrt{\sum_{k=1}^n (y_k^{i,m} - \bar{y}^{i,m})^2 \sum_{k=1}^n (y_k - \bar{y})^2}} \quad (23)$$

where $y_k^i$ represents a highly correlated particle path and $y_k^{i,m}$ represents the path of the newly selected particle.

Through such a particle selection method, the problem of particle depletion and data distortion can be effectively solved. Compared with the traditional particle filter algorithm, the Pearson coefficient-based particle filter can be

H. Liu *et al.*: Application Research of an Array Distributed IMU Optimization Processing Method in Personal Positioning

**IEEE** *Access*

continuously amplified by the high-quality features of the high-quality particles obtained by observation variables. And then we could make it closer to the real state.

### 5) NAVIGATION DATA ERROR ESTIMATION PROCESS IN PEARSON COEFFICIENT PARTICLE FILTER METHOD

The error estimation accuracy of particle filtering depends on whether the particles can fully cover the state features in pedestrian positioning. The method proposed in this paper uses the Pearson coefficient to measure the degree of agreement between the observation path of the particle and the path of the real state observation in the system. In other words, the particle whether can express the true state of the system, and finally provide an accurate error estimate.

The Pearson coefficient particle filtering process is mainly composed of five parts: 1. particle initialization; 2. importance density function sampling particle; 3. reselecting the path and the particle close to the real state; 4. calculating the importance function; 5. calculating the coefficient of re-sampling.

The particle filter process model is expressed as follows:

1) Particle initialization: $x_0^i \pi_0(dx_0), i = 1, 2, \ldots, N$

2) Sampling particles by the transfer function as an importance density function: $x_0^i P(x_k | x_{k-1}^i), i = 1, 2, \ldots, N$

3) Reselect the particles whose path is close to the real state. And the sampling process is: $x_k^{i,m} \cdot x_k^i, m = 1, 2, \ldots, M$, calculate the Pearson coefficient function: $S_k^{i,m}$, Assign the value: $x_k^i = x_k^{i,m}$, where the Pearson coefficient $S_k^{i,m}$ of $x_k^{i,m}$ is closest to 1.

4) Calculate the particle weight of the importance function: $\omega_k^i = P(y_k | x_k^i), i = 1, 2, \ldots, N$; normalize the particles' weight: $\omega_k^i = \omega_k^i / \sum_{j=1}^{N} \omega_k^j$;

5) Calculate $N_{eff} = (\sum_{i=1}^{N} (\omega_k^i)^2)^{-1}$.

If $N_{eff} < N_{thr}$, $[x_k^i, \omega_k^i]_{i=1}^{N} = \text{resampled}[x_k^i, \omega_k^i]_{i=1}^{N} i = 1, 2, \ldots, N$. The status value after re-sampling is $\hat{x}_k = \sum_{i=1}^{N} x_k^i \omega_k^i$.

## IV. THE COMPARISON RESULT OF SIMULATION

### A. FILTERING NOISE REDUCTION

At present, the commonly used filters for processing gyro signals are FIR, IIR, and the wavelet threshold methods. The FIR filter has good stability and linear phase characteristics. But due to its high order, there is a problem of delay. The primary advantage of the IIR filter is that it achieves better filtering at the same order. However, one disadvantage of the IIR filter method is that the phase characteristics of the filter cannot be controlled. A big problem encountered in the adaptive IIR filter designing is that the filter is unstable. Because the poles are scattered outside the stable area. The wavelet threshold filter has good stability and real-time performance. But due to the threshold itself, there will always be local oscillation and a certain deviation from the actual signal.

Aiming at the above problems, we designed a comparison test: the filter noise reduction test is performed by the collected dynamic gyro data. And the results through wavelet

**TABLE 1.** Comparison of filter noise reduction output results.

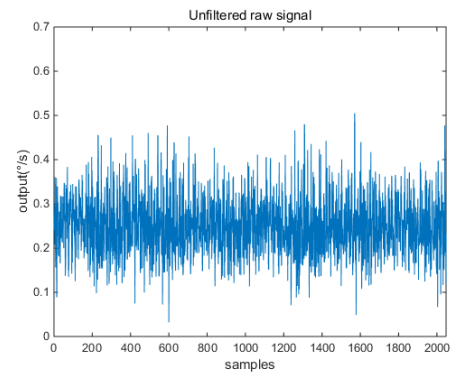| Filtering method | SNR (Signal to Noise Ratio) | Mean square error |
|---|---|---|
| Wavelet threshold filter | 39.7442 | 0.0137 |
| FIR filter | 36.1737 | 0.0173 |
| IIR filter | 32.3239 | 0.0226 |
| Proposed method | 43.1366 | 0.0074 |



**FIGURE 9.** The original signal diagram of Gyro dynamic output.
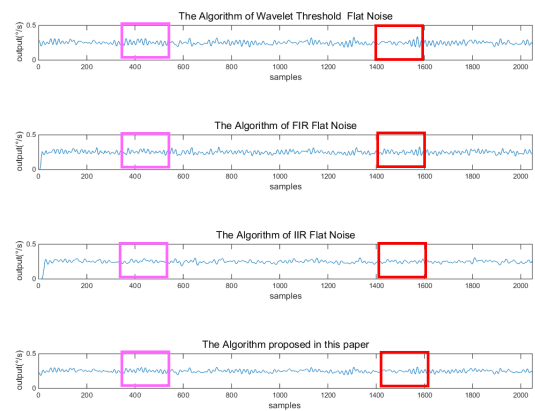


**FIGURE 10.** The comparison chart of filter noise reduction method.

threshold filter, FIR filter and IIR filter were respectively compared with the proposed method's effect. The original signal diagram is shown in Fig. 9. The filter noise reduction result by the above methods is shown in Fig. 10. And the filter result data is as shown in Table 1 below.

It can be seen from the pink and red boxes that the wavelet threshold filter always has a certain deviation compared to the other three methods; the FIR filter and the IIR filter can be seen the output values of these two methods are different from the original signal from the zero point, and there is a delay phenomenon. From the signal-to-noise ratio and the mean square error, we can get that the proposed method effectively improves the signal-to-noise ratio, and the mean square error is much smaller than other methods. In other words, this means that the output signal processed by this method is of good quality and is closer to the real state signal. Therefore, the method proposed in this paper just makes up for the above

**IEEE** *Access*

H. Liu *et al.*: Application Research of an Array Distributed IMU Optimization Processing Method in Personal Positioning

**TABLE 2.** Comparison of particle filter estimation results.

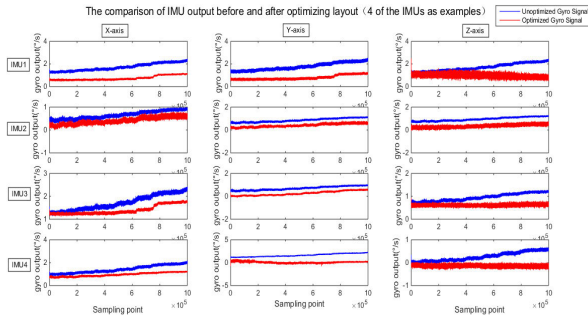| System state estimation method | Estimated accuracy |
| --- | --- |
| Traditional particle filtering method | 80% |
| Particle filter method proposed in this paper | 99% |



**FIGURE 11.** The comparison of IMU output before and after optimizing layout(4 of the IMUs as examples).

problem, and the output waveform is smoother and closer to the real signal waveform, which has certain superiority and goodness.

### B. OPTIMIZED LAYOUT

Using ANSYS for thermodynamic simulation, we could obtain the optimal layout and find its good heat dissipation effect. The 8 IMUs were placed according to the optimized layout and made into the circuit board. Then the thermostat experiment was carried out. Since the gyro output in the IMU is most affected by temperature, the inertial output data of the three-axis gyro was selected for experiment. The gyro data per axis was collected for 90 minutes. The temperature range was −20 °C to 40 °C, and the temperature difference value was 10 °C. The experimental results are shown in Fig. 11. It can be seen that after the optimal layout, the 4-channels three-axis gyro drift is significantly lower than before optimization. This shows that the optimized layout has a good effect in practical engineering applications.

### C. PARTICLE FILTER

The Pearson coefficient function was used to control the distribution of particles. When the particles were far away from the actual state real values, the particles were regenerated by the calculation of the Pearson coefficient function to ensure that all particles were close to the real state. Thus, we could solve the degradation and depletion problems of the particles. The estimated results are shown in Table 2.

Compared with the traditional particle filter algorithm, it can be seen from Fig. 14 that the proposed method can better estimate the real state of the system. When the real state of the system jumps in the pink box, the estimation error of the traditional method is larger. The method of this paper can effectively estimate error and follow the real state. Therfore, the Pearson coefficient particle filter algorithm can effectively improve the filtering accuracy.
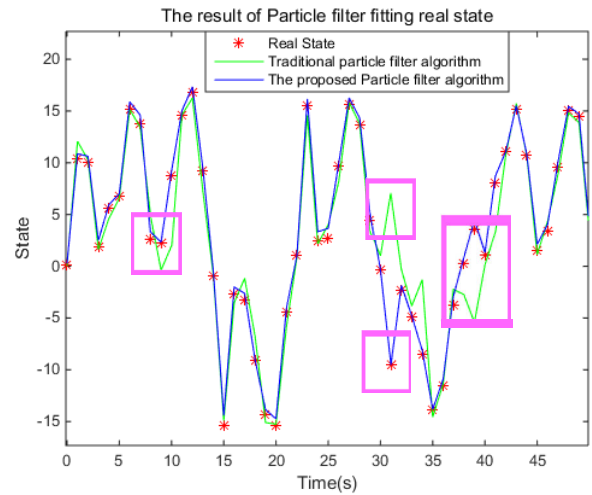


**FIGURE 12.** The comparison diagram of traditional particle filter and the particle filter proposed in this paper.



**FIGURE 13.** Experimental equipment.

## V. POSITIONING TEST AND RESULT ANALYSIS

### A. DESIGN OF THE POSITIONING TEST

In order to verify the true validity of the proposed method, the wearable positioning module independently studied by our laboratory is used, and the experimental equipment is shown in Fig. 13.

Experimental scene: Two sets of environment personal positioning experiments in large-span and blind were conducted at the National Defense Science and Technology Park of Beijing Institute of Technology. The first group consisted of a large-span closed-loop path in an underground garage with a length 287 m and width 184 m. The test time was 65 minutes. In the second group, in the No. 6 building with 17 floors and a vertical height of 70 meters, a large-span experiment was conducted on the upper and lower floors, and the experiment time was 68 minutes and 35 seconds (including the middle stop). The real validity of the proposed method is verified by the experimental environment of horizontal and vertical span. The track is shown in Fig. 14.

The wearable positioning terminal is mainly composed of 8 low power IMUs. The performance of a single IMU is shown in the following Table 3:

### B. RESULT ANALYSIS

#### 1) ACTUAL POSITIONING RESULT

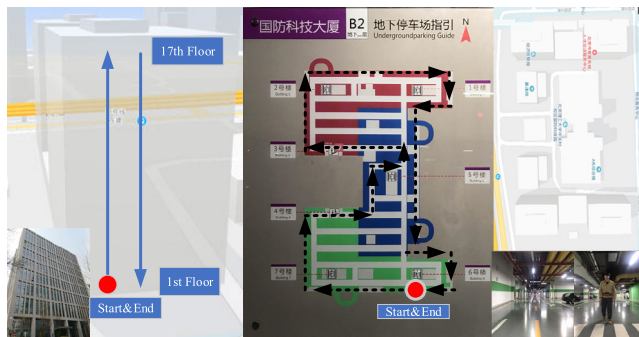In the experimental scene, the experimental results of the underground garage are shown in Figure 15-19. The purpose

H. Liu *et al.*: Application Research of an Array Distributed IMU Optimization Processing Method in Personal Positioning

**IEEE** *Access*



**FIGURE 14.** Experimental scene route diagram.



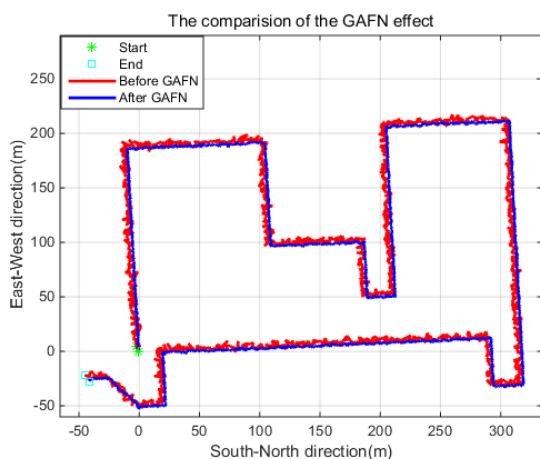**FIGURE 15.** The comparison of the GAFN algorithm effect.

**TABLE 3.** Inertial devices core parameters in IMU.

| Parameter | Parameter value |
|---|---|
| Endurance | 3h~4h |
| Operating Voltage | 3.3V |
| Working current | <0.2A |
| Working temperature range | -40℃~85℃ |
| Optimum working temperature | 25℃ |
| Gyro mechanical frequency | 25~29KHz |
| Gyro start-up time | 35ms |
| Gyro full scale | ±1000°/s |
| Gyro nonlinearity | ±0.1% |
| Accelerometer start-up time | 30ms |
| Accelerometer full scale | ±16g |
| Accelerometer nonlinearity | ±0.5% |

of the horizontal large-span underground garage is to verify the practical application of each innovation in this paper.

As shown in Fig. 15, after the algorithm proposed in this paper filters and denoises the sensor, it can be seen from the figure that the trajectory after noise reduction is more smooth. The signal-to-noise ratio before and after filtering noise reduction is 26.132 and 43.275, and the mean square error is 0.097 and 0.006.
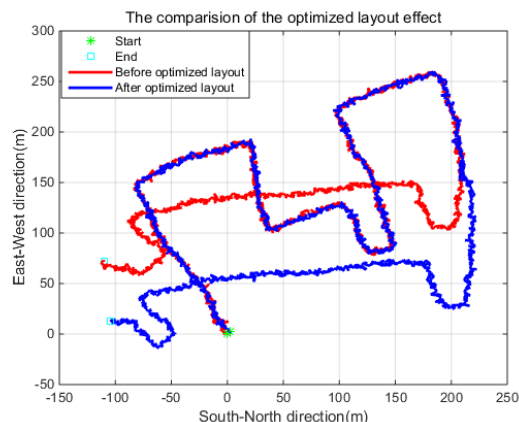


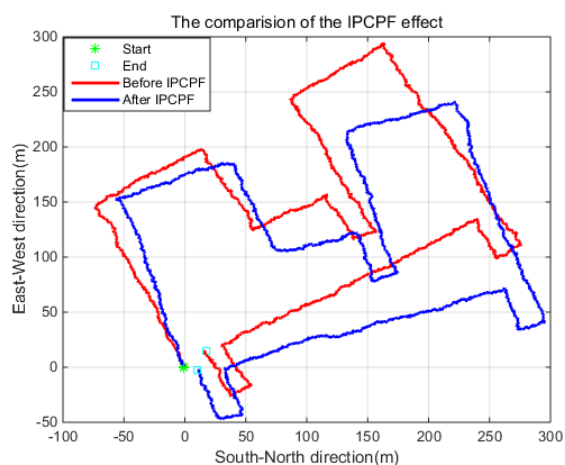**FIGURE 16.** The comparison of the optimized layout effect.



**FIGURE 17.** The comparison of the IPCPF algorithm effect.

As shown in Fig. 16, after re-arranging the heat generating unit, the influence of temperature on the inertial component under long-term positioning is reduced, and it can be seen that the divergence of the heading is effectively suppressed, but there is still a problem of heading offset. The positioning error results before and after the layout are 133.1126 meters and 102.4265 meters (TTD = 8.5%).

As shown in Fig. 17, the particle filter algorithm proposed in this paper can better observe the real state of the system and effectively estimate the system error. It can be seen that the divergence of the heading is effectively suppressed and the positioning accuracy is improved. The positioning error results before and after particle filtering are 40.8798 meters and 11.0126 meters (TTD = 0.92%).

As shown in Fig. 18, in order to show the true validity and positioning effect of the proposed algorithm more intuitively, the experimental algorithms proposed in this paper are experimentally simulated. It can be seen from the experimental results graph that the proposed algorithm combines the process, the track is continuously optimized, and the positioning accuracy is gradually improved, which proves that the proposed algorithm has a good application effect for the large-span blind environment. Finally, the positioning
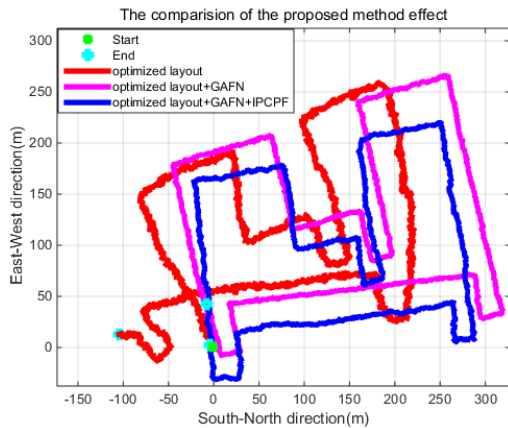
**IEEE** *Access*

H. Liu *et al.*: Application Research of an Array Distributed IMU Optimization Processing Method in Personal Positioning

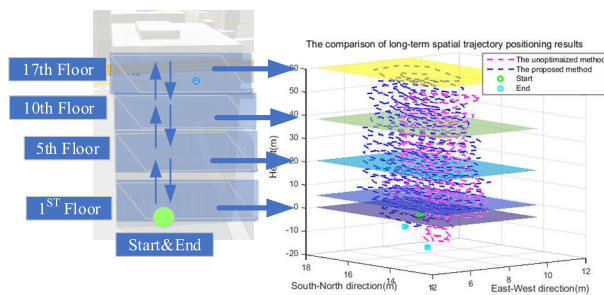**FIGURE 18.** The comparison of the proposed method effect.



**FIGURE 19.** The comparison of vertical large-span positioning results.

result after optimization layout proposed in this paper is 102.4265 meters. The positioning result of optimized layout and filtering noise is 16.5396 meters. The final positioning result of optimized layout and filtering noise and particle filtering proposed in this paper is 6.23 meters(TTD ≈ 0.52%).

As shown in Fig. 19, the proposed method is applied to the vertical large-span positioning effect as shown in the figure below. In this paper, the height error before and after the application of the optimization method is 13.21 meters and 4.56 meters. It can be seen that the method proposed in this paper also has a certain suppression on the high divergence of vertical large span.

### 2) ANALYSIS

Through vertical span and horizontal large span experiments, it can be seen that the proposed method has a certain optimization effect on the positioning effect of long-term blind environment. It can be seen from Fig. 15 that the GAFN can be effectively extracted by genetic optimization, and then the noise signal is inversely processed to complete the filtering process of the real signal. The experimental results show that the signal-to-noise ratio is effectively improved. The signal quality is good. It can be seen from Fig. 16 that, the influence of the heating of the main control unit on the gyro in the IMU, which is after the thermal optimization of the layout, is significantly reduced, so the layout optimization method proposed in this paper is real and effective. It can be seen

from Fig. 17 that the IPCPF can truly observe the state of the system, effectively suppress the heading divergence and correct the systematic error. It can be seen from Fig. 19 that in the application of vertical large span, the optimization method of this paper has a good effect on the positioning result. In the long-term upstairs process, the height does not cause divergence due to the long exercise time, but also goes upstairs. The first half of the process has good positioning accuracy. In the process of going downstairs, due to the accumulation of trial errors, a high degree of deviation occurs, but this is inevitable, but the method proposed in this paper has always been effective against the height deviation of the traditional navigation frame.

## VI. CONCLUSION

At present, most methods for improving the accuracy of pedestrian positioning are algorithm optimization and multi-condition detection to improve its effect. However, the positioning effect for the large span blind environment is not good. In order to achieve higher accuracy requirements and be useful in the mentioned above environment in the practical application of engineering, a solution to improve the synchronization of hardware and algorithms is urgently needed.

The above research and related experiments verify the optimized processing method of array distributed IMU in personal positioning. Firstly, the front-end data pre-processing and hardware layout of pedestrian navigation are used to solve the problems of delay, instability and fixed error in the general methods, and it has solved the impact of hardware system's heating on the whole positioning system in the large span blind environment, thus improving the data quality of the inertial sensor; by introducing the Fourier series to analyze the thermal resistance distribution of the circuit board, 8 IMUs are reasonably laid out on the basis of ensuring the working performance of the components. The maximum temperature of the core board is reduced by 3.537 °C, which is 4.23% lower than before optimization. And the average temperature is reduced by 2.83 °C. At the same time, reasonable temperature compensation is implemented for each IMU. It also improves and guarantees the quality of navigation data to some extent. In summary, the front-end processing provides a good and reliable data source for the post-solving part. In the back-end information fusion of the pedestrian navigation system, based on the common particle filtering method, the Pearson coefficient adapted to the high dynamic nonlinear system is introduced to effectively improve the inherent problems of particle degradation and particle depletion. The high-precision pedestrian positioning process in the large span blind environment is finally completed. After the above optimization, on the existing basis, The horizontal large-span positioning accuracy is only 6.23m (TTD ≈ 0.52%), and the vertical large-span positioning accuracy is only 4.56m (TTD ≈ 7.6%).

In the process of research and experiment, we also found the problems that need to be improved in the future research plan: for example, the application of the noise reduction

H. Liu *et al.*: Application Research of an Array Distributed IMU Optimization Processing Method in Personal Positioning

IEEE *Access*

algorithm requires a more accurate noise signal as a reference. And if the static noise signal is not accurate enough, the noise reduction effect will have an impact. At the same time, it is necessary to extract the static signals of multiple sensors to obtain the optimized sequence corresponding to them. The optimized sequence is not universal, and needs to be acquired for different sensors, which consumes a lot of time cost; the improved Pearson particle filter algorithm has a large performance improvement compared with the traditional particle filter, but there is still some deviation in the estimation of the real system error. It is necessary to increase the constraint conditions of observation channel and the measurement channel to improve the accuracy of their estimates in the following research.

## REFERENCES

[1] W. Yang, C. Xiu, J. Zhang, and D. Yang, "A novel 3D pedestrian navigation method for a multiple sensors-based foot-mounted inertial system," *Sensors*, vol. 17, no. 11, pp. 2695–2793, 2017.

[2] X. Tian, J. Chen, Y. Han, J. Shang, and N. Li, "A pedestrian navigation system based on MEMS inertial measurement unit," in *Proc. 35th Chin. Control Conf. (CCC)*, Chengdu, China, Jul. 2016, pp. 5325–5328.

[3] J.-O. Nilsson, A. K. Gupta, and P. Händel, "Foot-mounted inertial navigation made easy," in *Proc. Int. Conf. Indoor Positioning Indoor Navigat. (IPIN)*, Oct. 2014, pp. 24–29.

[4] X. Tian, J. Chen, Y. Han, J. Shang, and N. Li, "A novel zero velocity interval detection algorithm for self-contained pedestrian navigation system with internal sensors," *Sensors*, vol. 16, no. 10, p. 1578, 2016.

[5] Z. Liao, L. Song, P. Chen, and S. Zuo, "An automatic filtering method based on an improved genetic algorithm—With application to rolling bearing fault signal extraction," *IEEE Sensors J.*, vol. 17, no. 19, pp. 6340–6349, Oct. 2017.

[6] X. Dai and M. Bikdash, "Trend analysis of fragmented time series for mHealth apps: Hypothesis testing based adaptive spline filtering method with importance weighting," *IEEE Access*, vol. 5, pp. 27767–27776, 2017.

[7] L. Xiao-Guang, H. Jing-Tao, and G. Lei, "Micro mechanical gyro denoising method based on improved wavelet threshold," *J. Chin. Inertial Technol.*, vol. 22, no. 2, pp. 233–236, 2014.

[8] X. Tian, J. Chen, Y. Han, C. Song, and L. Yang, "Application of optimized wavelet threshold de-nosing method in pedestrian navigation system," *J. Chin. Inertial Technol.*, vol. 23, no. 4, pp. 442–445, 2015.

[9] L. Xiaobo, C. Guangwu, and W. Di, "Analysis and compensation of drift and noise in MEMS gyroscope," *Chin. J. Sens. Actuators*, vol. 31, no. 3, pp. 368–373, 2018.

[10] G.-X. Liu, L.-F. Shi, G.-W. Li, and L.-Y. Cheng, "Tri-adaptive method for improving the resolution of MEMS digital sensors," *IEEE Trans. Ind. Electron.*, vol. 66, no. 10, pp. 8189–8196, Oct. 2019.

[11] T. Shaoxin, S. Zhong, and M. Xiaofei, "Thermal layout optimization of incompletely arrayed electronic components," *Electron. Compon. Mater.*, vol. 31, no. 8, pp. 69–71, 2012.

[12] D. Wen-Xiong, T. Pu-Ying, and W. Shu-Bing, "3D-IC thermal analysis based on the finite element model," *Electron. Des. Eng.*, vol. 10, pp. 79–82, Oct. 2015.

[13] Z. Su, N. Liu, and Q. Li, "Error model and compensation of bell-shaped vibratory gyro," *Sensors*, vol. 15, no. 9, pp. 23684–23705, 2015.

[14] W. Wei and C. Xi-Yuan, "Modeling and compensation method of FOG temperature drift based on multi-scale and improved support vector machine," *J. Chin. Inertial Technol.*, vol. 24, no. 06, pp. 793–797, 2016.

[15] Z. Xu, S. Zhong, and M. Xiaofei, "Research on bias compensation of MEMS gyroscope under large temperature difference," *Chin. J. Sens. Actuators*, vol. 25, no. 8, pp. 1079–1083, 2012.

[16] D. Gang, "MEMS-IMU error analysis compensation method and experiment research," Ph.D. dissertation, Dept. Electron. Eng., Tsinghua Univ, Beijing, China, 2011.

[17] L. Chao, S. Zhong, and Z. Jialin, "A research about zero velocity trigger algorithm used in the wearable autonomous positioning technology," *Chin. J. Sens. Actuators*, vol. 27, no. 5, pp. 627–632, 2014.

[18] I. Skog, J.-O. Nilsson, and P. Handel, "An open-source multi inertial measurement unit (MIMU) platform," in *Proc. Int. Symp. Inertial Sensors Syst. (ISISS)*, Laguna Beach, CA, USA, Feb. 2014, pp. 97–100.

[19] J. A. Hidalgo-López, J. Romero-Sánchez, R. Fernández-Ramos, J. F. Martín-Canales, and J. F. Ríos-Gómez, "A low-cost, high-accuracy temperature sensor array," *Measurement*, vol. 125, pp. 425–431, Sep. 2018.

[20] I. Skog, J.-O. Nilsson, and P. Handel, "Pedestrian tracking using an IMU array," in *Proc. IEEE Int. Conf. Electron., Comput. Commun. Technol. (CONECCT)*, Jan. 2014, pp. 1–4.

[21] J. Y. Chang and A. Gupta, "Estimating the thermal interaction between multiple sideby-side chips on a multi-chip package," *Electron Cooling*, vol. 20, no. 2, pp. 1–3, May 2014.

[22] J. Galloway and T. Okpe, "Challenges in measuring theta JC for high thermal performance packages," *Electron Cooling*, vol. 20, no. 2, pp. 72–76, May 2014.

[23] D.-L. Chen, T.-C. Chen, P.-F. Yang, and Y.-S. Lai, "Thermal resistance of side by side multi-chip package: Thermal mode analysis," *Microelectron. Rel.*, vol. 55, no. 5, pp. 822–831, Apr. 2015.

[24] T. Cheng, X. Luo, S. Huang, and S. Liu, "Thermal analysis and optimization of multiple LED packaging based on a general analytical solution," *Int. J. Therm. Sci.*, vol. 49, no. 1, pp. 196–201, Jan. 2010.

[25] W. Jiao, S. Zhong, and Z. Yuexia, "Thermal layout optimization of handheld jammer with Fourier series," *Mod. Electron. Techn.*, vol. 39, no. 19, pp. 131–135, 2016.

[26] E. Foxlin, "Pedestrian tracking with shoe-mounted inertial sensors," *IEEE Comput. Graph. Appl.*, vol. 25, no. 6, pp. 38–46, Nov. 2005.

[27] S. Qiu, Z. Wang, H. Zhao, K. Qin, Z. Li, and H. Hu, "Inertial/magnetic sensors based pedestrian dead reckoning by means of multi-sensor fusion," *Inf. Fusion*, vol. 39, pp. 108–119, Jan. 2018.

[28] M. G. Puyol, P. Robertson, and O. Heirich, "Complexity-reduced Foot-SLAM for indoor pedestrian navigation," in *Proc. Int. Conf. Indoor Positioning Indoor Navigat. (IPIN)*, Sydney, NSW, Australia, Nov. 2012, pp. 1–10.

[29] Z. Qing-Hua, W. Jun-Wei, and L. Jian-Ye, "Heading compensation algorithm based on cellular structure particle filter for pedestrian navigation," *J. Chin. Inertial Technol.*, vol. 22, no. 5, pp. 576–579, 2014.

[30] Z. Gong-Yuan and Z. Zhong, "Overview of particle filter and its applications in integrated navigation system," *J. Chin. Inertial Technol.*, vol. 6, pp. 91–94, Jun. 2006.

**HENGZHI LIU** received the B.S. degree in electrical engineering and automation from the China University of Mining and Technology, Beijing, China, in 2017. He is currently pursuing the M.S. degree with the School of Automation, Beijing Information Science and Technology University. His research interests include navigation control and personal inertial navigation.

**QING LI** received the B.S. and M.S. degrees from the Department of Automation, Beijing Institute of Technology, Beijing, China, in 1983 and 1989, respectively, and the Ph.D. degree in aircraft design from the China Academy of Launch Vehicle Technology, Beijing, in 2003. She is currently a Professor with the Beijing Information Science and Technology University. Her research interests include inertial device, inertial navigation, and intelligent control of vehicle.

**IEEE** *Access*

H. Liu *et al.*: Application Research of an Array Distributed IMU Optimization Processing Method in Personal Positioning

**CHAO LI** received the B.S. degree in automatic control and the M.S. degree in control engineering from Beijing Information Science and Technology University, Beijing, China, in 2012 and 2015, respectively. He is currently pursuing the Ph.D. degree in navigation guidance and control with the School of Automation, Beijing Institute of Technology. His main research interests include inertial devices, signal processing, and inertial navigation.

**HUI ZHAO** received the B.S. degree in intelligent science and technology and the M.S. degree in navigation guidance and control from Beijing Information Science and Technology University, Beijing, China, in 2014 and 2017, respectively. He is currently pursuing the Ph.D. degree with the School of Automation, Beijing Institute of Technology. His research interests include attitude estimation of high spinning projectiles, integrated navigation, and personal inertial navigation.

• • •